Bull. Nat'l Taiwan Nor.Univ.
Vol. 38. pp.65-88 (1993)

師大學報
第38期 第65-88頁 (民國82年)

On the Recovery of Quadric Surface Shapes via Simultaneous Boundary and Surface Fitting

Greg C. Lee

Department of Information and Computer Education,
National Taiwan Normal Univerisity

Abstract

A method is proposed for detecting the shape of small parts of objects from fused intensity and range data. My primary assumptions are: (1) the most telling object features occur on the object rim and at object creases, and (2) occlusion existing in complex scenes requires the reconstruction of sensed objects in terms of these small parts. A fitting method that simultaneously fits specific quadric forms to both surface and contour data at object limbs or creases is presented. Fitting equations for spherical, cylindrical and conical limbs and for polyhedral creases are derived. Results from Monte Carlo experiments support the hypotheses that (1) fitting both surface and contour is superior, in terms of the quaality of the fit, to either surface fitting or contour fitting alone; (2) the shape of the surface is less likely to be misclassified when we use the proposed fused data fitting method.

1 Introduction

In order to understand the image of a scene, a system must ultimately be able to interpret parts of the sensed data as parts of objects. This is true regardless of whether the system is model-directed (top-down control)or data-directed (bottom-up control). Therefore, one of the most crucial issues in computer vision is the definition of scene primitives which are the goal of lower-level vision routines and the basis for higher levels of scene understanding. Not only is description of such primitives a challenging problem, but also is the definition of procedures for the extraction of primitives from sensed data.

We have proposed a new method for the detection of object primitives in *fused intensity-range data via simultaneously fitting intensity contours and the adjacent range (surface) data* [16] . Object primitives are taken to be patches of object surface at the object silhouette (rim) or at creases of the object. Such primitives thus give rise to observable 2D contours in the intensity image in addition to providing directly observable 3D shape in a range or depth image. In previous work, we have called these primitives *wings* [5] . We reason that such wings are more appropriate than larger granules such as generalized cylinders [19] or superquadrics [21] , because they will still be observable given large amounts of occlusion or other fragmentation caused by scene clutter.The quadric form and its projection are proposed for modeling wings at the object rim. An example scenario of how detected wings are used in higher level scene analysis is shown in Figure 1. Wing primitive are extracted (in parallel)for many windows of the sensed data. A grouping process is then applied toward creation of the next higher level representation, which is a line drawing labeled with shape features from the primitives and their composition. The labeled line drawing would then support model-based analysis or perhaps provide the final representation for grasping, navigation, or learning tasks.

This paper concentrates on the fused data fitting aspect of the wing detection process. Surface and contour fitting have their own advantages and disadvantages. We propose to combine the two and perform surface fitting in the presence of image contour constraints. For example, the limb boundary of a circular cylinder will be detected as much by its straight boundary contour as by its constantly curving surface points. Instead of using the general quadric surface equations for fitting, we have derived the implicit equations for planar,cylindrical , spherical and conical surfaces in general position as well as the 2D equations of the image contours of these surfaces. With the explicit quadric surface/contour models, the exact distance between a data point and the surface/contour model can be computed. Monte Carlo experiments are conducted to compare the proposed fused data fitting technique against fitting either the surface or contour data alone. The results indicate that fused data fitting is indeed superior.

2 Related Work

Many surface fitting techniques have been proposed in the past for detecting primitive shapes. Most involve minimizing some criterion function which usually is the assumed underlying model. For example, Flynn and Jain [8] fitted an implicit quadric equation specific to each surface type, using the Levenberg-Marquardt nonlinear least squares algorithm, and showed that fitting performs poorly if moderate noise is present.The well known RANSAC [7] algorithm is insensitive to gross error but is slower than the standard fitting methods.Others that find the best fitting quadric surface to the 3D points in a surface patch include [6, 10, 20] .The fit is typically performed by a least squares technique which uses only surface data and is sensitive to noise, especially when the general quadric form of 9 parameters is used and only a fraction of the surface form is observed. Cao, et. al. [4] recently completed a study comparing various quadric fitting methods for range data. They concluded that least squares surface fitting methods are feasible only if (1) sample rangels are well distributed on the surface, (2) noise is normally distributed, and (3) noise level is low.

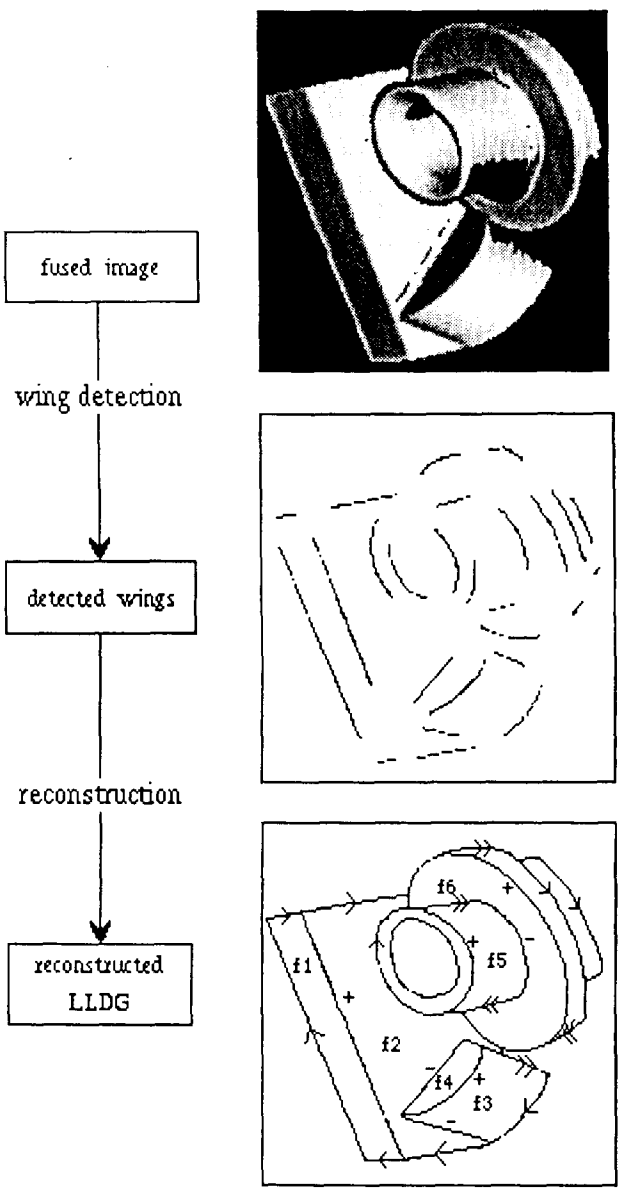

Figure 1: Sketch of proposed wing detection algorithm

Instead of surface fitting, Kriegman and Ponce [13] worked on contour fitting. Implicit equations of the image contours of the models (surfaces of revolution) are derived using Elimination theory. Equations are then fitted to the measured contour points. Objects are recognized by comparing the errors of fit of the various models. Fitting results on quality hand-segmented edgels were encouraging but fitting using noisy contour edgels were not reported. Also, the derived implicit equations are high-degree polynomials of many terms and a large amount of data points are required. If viewed against the paradigm of Ponce and Kriegman, the work done here explores solutions with a minimal number of parameters and a minimal amount of observed data.

Surface fitting has traditionally been done by fine tuning the parameters of an underlying assumed surface model and edge constraints are usually not used. However, edge information from objects provides strong clues about the local shape of surfaces [12].For example, Lowe used only 2D contours for the recognition of objects in general position [17];furthermore, superquadrics surface fitting with edge constraints has been successfully demonstrated by Bajcsy and Solina [1].More recently, Lowe [18],Taubin [24], and Bolle *et al.* [3] have also demonstrated the importance of contour information by utilizing it in estimating initial parameters prior to fitting and/or using it to aid the recovery of parameters during fitting.

3 Approach to Fitting Fused Data

Conceptually, fitting both surface and contour data would require two fitting models: a surface model and a contour model.Consequently, 2 fitting functions P_{3d} and P_{2d} are needed.If the two models have two mutually distinct sets of parameters, then fitting can be performed individually. But this would defeat the purpose of having intensity contour data which is to aid the recovery of the surface parameters.In Section 3.1 , we shall show how to derive the equation of the orthographic projection of the limb edge from the general quadric surface equation.

In so doing, we will force the two equations to have the same set of parameters.

Fitting the general P_{3d} and P_{2d} equations to fused data, which have many complex terms, is computationally expensive [13].Furthermore, the error model for computing the distance between the fitted model and the data points can only be approximated in practice [4,13].Our approach is to fit explicit categorical surface models and their respective limb projections to fused data.With explicit surface models, we are able to derive and use the exact distance between the data points and the model as the residual function in evaluating the goodness of fit.Moreover, there are fewer parameters to fit.

In Section 3.2, we shall give the P_{3d} and the derived P_{2d} limb projection equations of spherical, cylindrical and conical models. We will also list the equation of the projection of the crease edge formed by two planar surfaces. Equations of the crease edges formed by other surfaces can be found in [15]. This is followed by the derivations of the exact distance functions from a data point to each of the surface and contour models.

3.1 Derving P_{2d} from P_{3d}

In the following derivation, the coordinate frame(x,y,z) is assumed to be camera-centered and that parallel projection is also assumed.

The general equation of a quadric surface takes the form of

$$P_{3d}(x,y,z)=ax^2+by^2+cz^2+dxy+exz+fyz+gx+hy+iz+j=0. \qquad (1)$$

To find the equation of the projection of the limbs, We must identify the points belonging to the limb boundary.Note that a point on the quadric surface is on the limb if and only if the surface normal at that point is orthogonal to the projection direction.The surface normal at a given point (x,y,z) is simply

$$N_{P_{3d}}(x,y,z)=\left(\frac{\partial P_{3d}}{\partial x},\frac{\partial P_{3d}}{\partial y},\frac{\partial P_{3d}}{\partial z}\right).$$

If we assume that the viewing direction is along the z-axis and that the viewpoint is at $(0,0,z_v)$, the projection direction for a given point (x,y,z) is then

$$P_{proj}(x,y,z)=(x,y,z-z_v).$$

Thus, the limbs must lie on the surface defined by the planar equation

$$P_{proj} \cdot N_{P3d}=x(ez_v+g)+y(fz_v+h)+z(2cz_v+i)+(iz_v+2j)=0. \quad (2)$$

Finally, by solving Equation 2 for z in terms of x and y and substituting back into Equation 1 and taking the limit as $z_v \rightarrow \infty$, we arrive at P_{2d}, which is the equation of the limb, *orthographically* projected onto the image plane. The P_{2d} equation derived from a general P_{3d} surface equation is long and is omitted here. It should be noted that only simple algebraic manipulations are needed in deriving the final form.

3.2 P_{3d}s and P_{2d}s of Explicit Quadric Surface Models

Using the above procedure, we have derived the equations of the orthographic projections of the limb boundaries of spherical, cylindrical and conical surfaces.

Spherical Surfaces

A sphere in general position has the equation

$$P_{3d}^{sph}(x,y,z;x_0,y_0,z_0,r_0)=(x-x_0)^2+(y-y_0)^2+(z-z_0)^2-r_0^2=0 \quad (3)$$

There are four parameters: three translational$(x_0,y_0,z_0)$and radius r_0. It is obvious that the orthographic projection of the contour is a circle. By applying the procedure outlined above, we arrive at the equation of this circle.

$$P_{2d}^{sph}(x,y,z;x_0,y_0,r_0)=(x-x_0)^2+(y-y_0)^2-r_0^2=0 \quad (4)$$

Note that only three of the four P_{3d}^{sph} parameters are present in P_{2d}^{sph}. This means that fitting P_{2d}^{sph} to contour points leaves one free parameter(*i.e.*,z).

Cylindrical Surfaces

The circular cylindrical model has 5 parameters: two translational(x_0,y_0), two rotational$(\alpha,\beta)$and the radius(r_0).We derived P_{3d} for the cylindrical model as follows.Take a cylinder with radius r_0 and the axis coincident with the z-axis. Translate the cylinder along the x-axis by x_0 and along the y-axis by y_0 Using $(x_0,y_0,0)$ as the origin of the new coordinate frame, rotate about the x-axis by angle α and then rotate about the new y-axis by angle β. The implicit quadric

equation of the cylinder in the new position can then be expressed in the original coordinate frame as:

$$P_{2d}^{cyl}(x,y,z;x_0,y_0,r_0,\alpha,\beta)=((y-y_0)cos(\alpha)+zsin(\alpha))^2+$$
$$((x-x_0)\,cos(\beta)+(y-y_0)sin(\alpha)sin(\beta)-z\,cos(\alpha),sin(\beta))^2-r_0^2 \qquad (5)$$

The orthographic projection of the limbs are two straight lines. The P_{2d} derived using the method outlined above is a quadric equation representing the two parallel lines.By solving one of the variables, we have the equation of each of the lines.

$$P_{2d}^{cyl}(x,y;x_0,y_0,r_0,\alpha,\beta)=(x-x_0)\,(cot(\beta),sin(\alpha))+(y-y_0)\pm$$
$$\frac{\sqrt{r_0^2(6-2cos(2\alpha)-cos(2(\alpha-\beta))-2cos(2\beta)-cos(2(\alpha+\beta)))^3csc(\beta)^2}}{2^{\frac{9}{2}}(sin(\alpha)^2+cos(a)^2sin(\beta)^2)}$$

Conical Surfaces

The circular cone model has 6 parameters: three translational(x_0,y_0,z_0), two rotational angles (α,β) and the height of the cone at unit radius (d_0). To find the equation of the cone in general position, we first assume that the circular cone is in the upright position (*i.e.*, has its vertex at the origin and the axis coincident with the positive z-axis). By translating the cone along the x-, y- and z-axis by x_0,y_0,z_0, respectively, then rotating about the new x- and y-axis by α,β as in cylindrical case, we arrive at the equation of the cone in general position.

$$P_{3d}^{con}(x,y,z;x_0,y_0,z_0,d_0,\alpha,\beta)=U^2+V^2-W^2/d_0^2,$$
$$U=(x-x_0)cos(\beta)+(y-y_0)sin(\alpha)sin(\beta)-(z-z_0)cos(\alpha)sin(\beta)$$
where $V=(y-y_0)cos(\alpha)+(z-z_0)sin(\alpha)$
$$W=(x-x_0)sin(\beta)+(y-y_0)sin(\alpha)cos(\beta)+(z-z_0)cos(\alpha)cos(\beta)$$

After expanding and rewriting $P_{3d}^{con}as$

$$P_{3d}^{con}(x,y,z;x_0,y_0,z_0,d_0,\alpha,\beta)=ax^2+by^2+cz^2+dxy+exz+fyz+gx+hy+iz+j,$$

the derivation of the equation of the projection of the limb edges is straightforward.

$$P_{2d}^{con}(x,y,z;x_0,y_0,z_0,d_0,\alpha,\beta)=kx^2+ly^2+mxy+nx+oy+p,$$

where

$$k=a-\frac{e^2}{4c},\quad l=b-\frac{f^2}{4c},\quad m=d-\frac{ef}{2c}$$

$$n=g-\frac{ei}{2c},\quad o=h-\frac{fi}{2c},\quad p=j-\frac{i^2}{4c},$$

By comparing Equation 3.2 with the factoring of two linear equations, we can solve for the equation of each limb projection,namely

$$P_{2d_1}^{con}: y=\frac{\sqrt{m^2-4kl}-m}{2l}x+\frac{-\sqrt{o^2-4lp}-o}{2l} \tag{6}$$

$$P_{2d_2}^{con}: y=\frac{\sqrt{m^2-4kl}-m}{2l}x+\frac{-\sqrt{o^2-4lp}-o}{2l} \tag{7}$$

Two Planar Surfaces

Our equation of planar surfaces has three parameters (a, b, d) and takes the form of

$$P_{3d}^{pln}(x,y,z;a,b,d)=ax+by+z+d=0 \tag{8}$$

To find the equation of the projection of the crease edge between two intersecting planar surfaces, we simply take two such equations and set them equal to each other

$$P_{3d}^{pln_1}(x,y,z;a_1,b_1,d_1)=a_1x+b_1y+z+d_1=0$$

$$P_{3d}^{pln_2}(x,y,z;a_2,b_2,d_2)=a_2x+b_2y+z+d_2=0$$

$$P_{2d}^{pln+pln}(x,y;a_1,b_1,d_1,a_2,b_2,d_2)=(a_1-a_2)x+(b_1-b_2)y+(d_1-d_2)=0 \tag{9}$$

Note the resulting $P_{2d}^{pln+pln}$ equation is defined in terms of all six parameters that appear in $P_{3d}^{pln_1}$ and $P_{2d}^{pln_2}$. By fitting data points to P_{2d}^{pln}, we are in effect finding the parameters of the two intersecting planes.

3.3 New Residual Funtions

If we were to do least-squares fit on the fused data with the above implicit equations, then we would be minimizing the squared residual errors.It is well known that this residual error measure may be a poor indicator of the error between the data points and the fitted model [14] .

A better approach is to use the exact normal distance function when comput-

ing fitting errors. Instead of minimizing the squared residual errors, we have to minimize the sum of the squared normal distances between the data points and the fitted curve . Hence the quantity to be minimized is

$$\sum_{i=1}^{n} dist(x_i, P(x_i; \hat{\Omega}))^2$$

where χ_i denotes a data point and $\hat{\Omega}$ the set of parameters.

Unfortunately, the exact formulation of this normal distance between the data point and the fitted curve/surface does not often exist (*e.g.* determining distance between a 3D point and a general quadric surface). Some surface fitting algorithms in the computer vision community have either continued to use the residual errors [8] or used an approximation to the true normal distance function [2,11,13,23,24] . The study by Gross and Boult [9] showed that the *ad hoc* goodness-of-fits measures have many problems and biases in parameter fitting. It was shown that fitting superquadrics with an error measure based on the true Euclidean distance fares far better than if other *ad hoc* measures are used. Since we have modeled different types of quadric surfaces by their respective explicit quadric equations, we are able to derive the true normal distance functions. We shall denote the new residual functions as DP_{3d}^{qqq} and DP_{2d}^{qqq} where qqq denotes one of the surface/contour types. In the following, only the equations are given, the derivation can be found in [15] .

Planar.

$$DP_{3d}^{pln_1}(x,y,z;\ a_1,b_1,d_1) = \mid a_1x+b_1y+z+d_1 \mid ,$$

$$DP_{3d}^{pln_2}(x,y,z;\ a_2,b_2,d_2) = \mid a_2x+b_2y+z+d_2 \mid ,$$

$$DP_{3d}^{pln+pln}(x,y,z;\ a_1,b_1,d_1,a_2,b_2,d_2) = \left| \frac{P_{2d}^{pln+pln}}{\sqrt{1+\frac{(a_2-a_1)^2}{(b_1-b_2)}}} \right|$$

Spherical.

$$DP_{3d}^{sph}(x,y,z;\ x_0,y_0,z_0,r_0) = \mid \sqrt{(x-x_0)^2+(y-y_0)^2+(z-z_0)^2}-r_0 \mid ,$$

$$DP_{2d}^{sph}(x,y;\ x_0,y_0,z_0,r_0) = \mid \sqrt{(x-x_0)^2+(y-y_0)^2}-r_0 \mid .$$

Cylindrical.

$$DP^{cyl}_{3d}(x,y,z;x_0,y_0,r_0,(\alpha),\beta)=$$
$$(y_0-y)cos(\alpha)sin(\alpha)cos(\beta)^2+(x-x_0)cos(\alpha)cos(\beta)sin(\beta)-$$
$$(\frac{1}{(sin(\alpha)^2+cos(\alpha)^2sin(\beta)^2)})((sin(\alpha)^2+cos(\alpha)^2sin(\beta)^2)r^2+$$
$$2(-x^2+2xx_0-x_0^2)cos(\alpha)^2cos(\beta)sin(\alpha)sin(\beta)+$$
$$2(-xy+x_0y+xy_0-x_0y_0)sin(\alpha)sin(\beta)cos(\beta)+$$
$$(-y^2+2yy_0-y_0^2)(cos(\alpha)^4+sin(\alpha)^4)sin(\beta)^2+$$
$$2(-y^2+2yy_0-y_0^2)cos(\alpha)^2sin(\alpha)^2sin(\beta)^2)-z,$$
$$DP^{cyl}_{2d}(x,y,z;\ x_0,y_0,r_0,\alpha,\beta)=\left|\frac{P^{cyl}_{2d}}{\sqrt{1+cot^2(\beta)sin^2(\alpha)}}\right|.$$

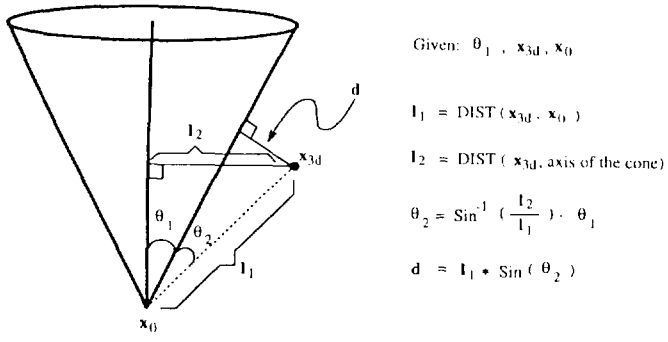

Figure 2: Computing the Euclidean distance from a point in 3D to the surface of a cone.

Conical.

We use Figurere 2 to help extract the new residual function for cones.

$$DP^{con}_{3d}(x,y,z;x_0,y_0,z_0,d_0,\alpha,\beta)=l_1 * sin(\theta_2)$$
$$DP^{con}_{2d}(x,y,z;x_0,y_0,z_0,d_0,\alpha,\beta)=\left|\frac{P^{con}_{2d}}{\sqrt{1+slope^2}}\right|,$$

where *slope* is the slope of the line P^{con}_{2d}.

4 Monte Carlo Experiments

Experiments were conducted to answer the following questions.

1.Is the combination of contour and surface data superior to either one used alone?

2.Can quadric surface patches be adequately differentiated using fused fitting?

In the first set of experiments, we set out to evaluate the quality of the fit on planar, spherical, cylindrical and conical surfaces when using respectively only contour data, surface data and fused data.True surface models were used during each fit.

While the first set of experiments used true surface/contour models during fitting, the second set of experiments fitted both true and incorrect models to the data points. The goal is to determine if the wrong models will fit the surface/contour patch better than the true model. In other words, the experiments are to explore the classification power of the fused data fitter against the usual techniques.

Table 1: Range (in inches) of parameters

Planar:	$-5.0 \leq a_1, b_1, d_1, a_2, b_2, d_2 \leq 5.0.$
Spherical:	$-5.0 \leq x_0, y_0 \leq 5.0;$ $15.0 \leq z_0 \leq 25.0;$ $1.0 \leq r_0 \leq 10.0.$
Cylindrical:	$-5.0 \leq x_0, y_0 \leq 5.0;$ $1.0 \leq r_0 \leq 10.0;$ $5.0 \leq \alpha, \beta \leq 175.$
Conical:	$-5.0 \leq x_0, y_0 \leq 5.0;$ $15.0 \leq z_0 \leq 25.0;$ $0.5 \leq d_0 \leq 2.0;$ $5.0 \leq \alpha, \beta \leq 175.$

One thousand Monte Carlo trials were performed in each of the experiments. During each iteration, a new set of surface and contour data were synthetically generated as follows.First the parameters of the surface model were generated randomly. The ranges from which those parameters were generated are given in Table 1. Points on the surface could then be rendered without error using the selected parameter values and the appropriate surface model equation.A rectangular sampling window of specified size was placed over the image contour of the limb boundary. In the case of two intersecting planes, the window was placed over the line in the image that corresponded to the crease edge in 3D. Surface and contour points for fitting were sampled from this window. The total number of points sampled in each of the trials was 30. For surface points, Gaussian noise was added to the z-component to simulate sensor errors. The results at two noise levels, $\sigma = 0.01$ and $\sigma = 0.05$ were studied. Gaussian noise at levels of $\sigma =$

0.002 and $\sigma = 0.01$ was also added to both x- and y-components of the contour data points. In reality, the noise level of our range scanner [25] was determined to have $\sigma < 0.01$. We also experimented at a higher σ because we feel that range data derived using shape-from-x techniques would have a much higher noise level

4.1 Fitting True Models to Contour, Surface, and Fused Data

The first four experiments involve fitting the true model to spherical, cylindrical, conical and planar surface patches.We compare the results of fitting fused (both contour and surface)data to fitting contour-only or surface-only data. The fused data consists of 15 points sampled from the contour and 15 points sampled from the adjacent surface patch for a total of 30points. For surface-only and contour-only data sets, 30 points were sampled from either the surface patch or the contour in the window.

Since true model parameter values are known,the initial parameter estimates are taken to be the truth plus/minus some random deviations having uniform distribution. Table 2 lists the range of deviations for all of the parameters.

Table 2: Initial estimate of the model parameters

Planar		Conical	
$\hat{a_1} = a_1 \pm \mathrm{d}a_1$,	$\mathrm{d}a_1 \sim U(0,1)$	$\hat{x_0} = x_0 \pm \mathrm{d}x_0$,	$\mathrm{d}x_0 \sim U(0,1)$
$\hat{b_1} = b_1 \pm \mathrm{d}b_1$,	$\mathrm{d}b_1 \sim U(0,1)$	$\hat{y_0} = y_0 \pm \mathrm{d}y_0$,	$\mathrm{d}y_0 \sim U(0,1)$
$\hat{d_1} = d_1 \pm \mathrm{d}d_1$,	$\mathrm{d}d_1 \sim U(0,1)$	$\hat{z_0} = z_0 \pm \mathrm{d}z_0$,	$\mathrm{d}z_0 \sim U(0,1)$
$\hat{a_2} = a_2 \pm \mathrm{d}a_2$,	$\mathrm{d}a_2 \sim U(0,1)$	$\hat{d_0} = d_0 \pm \mathrm{d}d_0$,	$\mathrm{d}d_0 \sim U(0,0.5)$
$\hat{b_2} = b_2 \pm \mathrm{d}b_2$,	$\mathrm{d}b_2 \sim U(0,1)$	$\hat{\alpha} = \alpha \pm \mathrm{d}\alpha$,	$\mathrm{d}\alpha \sim U(0,10)$
$\hat{d_2} = d_2 \pm \mathrm{d}d_2$,	$\mathrm{d}d_2 \sim U(0,1)$	$\hat{\beta} = \beta \pm \mathrm{d}\beta$,	$\mathrm{d}\beta \sim U(0,10)$
Spherical		**Cylindrical**	
$\hat{x_0} = x_0 \pm \mathrm{d}x_0$,	$\mathrm{d}x_0 \sim U(0,1)$	$\hat{x_0} = x_0 \pm \mathrm{d}x_0$,	$\mathrm{d}x_0 \sim U(0,1)$
$\hat{y_0} = y_0 \pm \mathrm{d}y_0$,	$\mathrm{d}y_0 \sim U(0,1)$	$\hat{y_0} = y_0 \pm \mathrm{d}y_0$,	$\mathrm{d}y_0 \sim U(0,1)$
$\hat{z_0} = z_0 \pm \mathrm{d}z_0$,	$\mathrm{d}z_0 \sim U(0,1)$	$\hat{r_0} = r_0 \pm \mathrm{d}r_0$,	$\mathrm{d}r_0 \sim U(0,2)$
$\hat{r_0} = r_0 \pm \mathrm{d}r_0$,	$\mathrm{d}r_0 \sim U(0,1)$	$\hat{\alpha} = \alpha \pm \mathrm{d}\alpha$,	$\mathrm{d}\alpha \sim U(0,10)$
		$\hat{\beta} = \beta \pm \mathrm{d}\beta$,	$\mathrm{d}\beta \sim U(0,10)$

The popular Levenberg-Marquardt non-linear least-square fitting scheme [22] are employed to fit the fused data.In studying the results of the experiments,one of the statistics reported is the total number of bad fits over the 1000 trials.A fit is considered bad if the computed χ^2 is over the threshold of 12. Since 30 data points were used in each trial, and the number of parameters is either 4 (spherical), 5 (cylindrical) or 6 (conical, planar),the degrees of freedom would then be 26, 25 or 24.A χ^2 of 12 with a number of degrees of freedom in the range of 24— 26 indicates that the probability of the fit obtaining a χ^2 as small as 12 happening by chance is about 2%.While a bad fit is a type II error in the hypothesis testing sense in which the correct hypothesis is falsely rejected,we note that additional reject conditions will be added later, making the term "type II error" an inaccurate description of the rejects by the whole model fitting procedure.Thus, we shall use the term "bad fits" to denote those fits that resulted in a type II error or rejected by the additional "good" fit criteria.

All other statistics are computed over the good fits only.Besides reporting the average and maximum deviations of the estimated parameters from the ground truth, We also report three other summarizing statistics. They are the average *d.lse* ,the average *m.lse* and the average number of iterations for the good fits to converge. The *d.lse* models the variance of the Gaussian noise in the data and is computed as the unweighted sum of the squares of the Euclidean distances between the data points and the fitted surface/contour averaged over all 30 points.The *m.lse* is a similar quantity except the error is computed from the data points *before Gaussian noise was added* to the fitted surface/contour. This measure gives an indication of how well the estimated surface/contour matches the noise free data.

For space consideration, we only present, in detail, the result of the experiment of fitting cylindrical model to sampled cylindrical data and only summarize the results of the other three experiments. Overall, the results suggest that simultaneously fitting surface and contour points can tolerate a much higher noise level. The fitted parameters are more accurate, and these results are obtained without much increase in computation time (one more iteration).

Table 3: Fitting Cylindrical Model on Cylindrical Data

Number of trials: 1000 Number of samples per trial: 30								
Parameter Measurements are in inches			Contour-Only		Surface-Only		Fused	
			Avg.	Max.	Avg.	Max.	Avg.	Max.
$\sigma = 0.01$		$\hat{x_0} - x_{true}$	1.69	61.84	0.29	14.52	0.12	2.81
		$\hat{y_0} - y_{true}$	0.44	5.33	0.17	5.27	0.08	1.92
		$\hat{r_0} - r_{true}$	0.25.	0.50	0.09	0.46	0.03	0.27
		$\hat{\alpha} - \alpha_{true}$	4.59	9.98	0.63	7.52	0.60	5.19
		$\hat{\beta} - \beta_{true}$	2.70	9.71	0.49	6.88	0.48	4.30
		χ^2	0.06889		0.26924		0.18603	
		d lse	0.00002		0.00009		0.00006	
		m lse	0.00002		0.00725		0.00067	
		iterations	3.45		7.18		6.63	
		bad fits	815		58		77	
$\sigma = 0.05$		$\hat{x_0} - x_{true}$	1.40	18.74	0.54	16.39	0.50	14.51
		$\hat{y_0} - y_{true}$	0.43	5.44	0.29	3.29	0.35	10.86
		$\hat{r_0} - r_{true}$	0.25	0.50	0.23	0.50	0.15	0.50
		$\hat{\alpha} - \alpha_{true}$	4.63	9.99	0.91	9.95	1.29	9.89
		$\hat{\beta} - \beta_{true}$	2.61	9.70	0.62	5.02	0.70	5.37
		χ^2	0.32513		6.63258		4.31621	
		d lse	0.00011		0.00221		0.00144	
		m lse	0.00003		0.00087		0.00369	
		iterations	3.72		4.76		6.18	
		bad fits	819		676		186	

Experiment 1: Cylindrical

The window from which the data points are to be sampled is a rectangular box of height $2.0r_0$ (running parallel to the axis of the cylinder) and width $0.6r_0$. This roughly covers 33%of the projected area of a cylinder of height 2.0,r_0.Here a fit is considerd good if and only if(1) $\chi^2 < 12.0$,(2) $| \hat{r}_0 - r_0 | \leq 0.5$,*and*(3) $| \hat{\alpha} - \alpha | \leq 10°$ *and* $| \hat{\beta} - \beta | \leq 10°$ Those conditions force a good fitted cylinder to have similar size and have the axis approximately pointing in the true direction.The Results from the Monte Carlo trials are summarized in Table 3.

Clearly, the fused fit out-performed the other two methods. This is especially true with the noisier data.Note that the contour-only based fitting converged on less than 20% of all trials performed and is therefore not a good choice for parameter estimations. Under light noise contamination, the convergence rate for the surface-only fit is 2% higher than the fused fit. However, the fused fits result in better parameter estimates and slightly faster rate of convergence. With a higher noise level, the surface-only fits failed much more frequently and the estimated parameters were inferior to those obtained in fused fits.

Experiment 2-4 : Spherical/Conical/Planar

The observations made in the cylindrical case also hold true in these experiments. In general, fuse fitting recovers the 3D object shape and pose parameters much better than when fitting range or 2D contour data along. In the spherical and the conical cases, the all important radius and the d_0 parameters were much closer to the true values even in the influence of noise. The range-only and the fused fitting methods functioned equally well when we applied them to the planar surface patch. This is not unexpected since many researchers have reported good fitting results with polyhedral objects. Our conlusion merely implies that fused fitting is not needed for polyhedra.

4.2 Surface Classification Experiments

The next 4 experiments are designed to test the surface classification and shape recognition power of fitting fused data as compared to fitting surface-only data. Specifically, we want to test how well the fused fits reject the fitting of one model to data generated from other models(*e.g.*, fitting all models to spherical surface patch).

The initial guesses of the parameter values are important in finding the correct fit. When the true model is fitted to the surface patch, the initial parameter estimates are perturbed from the truth as before. However, when an incorrect model is fitted, the initial estimate of the parameters can no longer be directly

generated from the true model parameters of data to be fitted. Care has been taken to ensure that the initial guess results in a surface close to the actual surface patches. The reported statistics include the number of bad fits, the average χ^2, the average number of iterations and 2 new entities. First, *Best* χ^2 counts the frequency in which one model is the best fit among it *all* good fits in terms of χ^2. If all models failed to fit a surface patch, then the comparison is not made.The other new entry, *misclassification %*, is the percentage in which the wrong surface model fitted the surface patch better then the true surface model. If all surface models failed to converge, then no classification was performed and that trial was not included in the calculation of frequency of misclassification.Again, detail results of only one set of experiment is given below. The rest are again only summarized.

Table 4: Fitting all models to Cylindrical surface patch

True surface form: CYLINDRICAL Number of trials: 1000 Number of points sampled per trial: 30									
		Surface-Only				Fused			
		con	cyl	sph	pln	con	cyl	sph	pln
σ || 0.01	*bad fits*	530	58	882	736	824	61	913	571
	χ^2	5.38	0.30	6.76	5.63	5.11	0.21	6.10	5.21
	iterations	23.72	6.80	8.53	3.61	29.00	6.82	4.55	3.41
	Best χ^2	58	905	6	13	4	933	0	40
	% misclassified	7.8%				4.5%			
σ || 0.05	*bad fits*	661	728	996	857	859	233	942	637
	χ^2	7.17	6.53	10.09	8.85	6.09	4.39	7.94	6.87
	iterations	21.16	5.43	4.00	3.63	29.10	6.51	4.67	3.45
	Best χ^2	276	235	1	87	45	706	0	96
	% misclassified	60.8%				16.6%			

Experiment 5: Fitting all models to Cylindrical patch

The cylindrical surface/contour data sets were generated as in Experiment 1 except for the height of the window (along the limb boundary) which was shrunk

from $2.0r_0$ down to $0.5r_0$.With the original elongated window, the spherical and conical models would be quickly ruled out by the long straight limb and zero curvature along the limb.With a more squared sampling window ($0.5r_0 \times 0.6r_0$), the conical and spherical models have a better chance of fitting the cylindrical surface patch and the contribution of the contour data in fused fitting can be better interpreted. The results of the experiments are given in Table 4.

With low Gaussian noise, the cylindrical model has the best fit most of the time. Although the misclassification rate for fused fits (4.5%)is lower than that of surface-only fits (7.8%), they are close. With higher noise level, the power of shape recognition with fused data is more apparent. While fitting surface-only data yields a 60.8%misclassification rate, fused data fitting has a much lower 16.6 % error rate. Furthermore, the conical model fitted the cylindrical surface patch more successfully than the cylindrical model when only surface points were used, but this tendency was reversed with fused data. This can be attributed to the fact that the Gaussian noise induced surface patch no longer resembles a cylindrical patch. Since a conical model has one more degree of freedom, it would fit this "irregular"surface patch better than the cylindrical model. When the limb contour is introduced in fused fitting, it forces the limb of the conical model to line up with the contour data and consequently makes the tapering surface of the conical model a bad fit to the non-tapering surface patch. On the other hand, the contour data put a fix on the axis direction of the cylindrical model which wasn't available to surface-only fitting.Consequently, it would fit better than before.

In fitting surface-only data set, when the surface is misclassified, the conical model tends to have the best fit, followed by planar then spherical models. We must note that although a large sphere may fit a small cylindrical patch well, we have made an explicit assumption that no sphere of radius greater than 10 inches is possible.Thus, all spherical fits with r_0>10 were rejected.

On the other hand, if the surface patch is misclassified when fitting fused data, the planar model tends to have the best fit followed by the conical model but never the spherical model.

Experiments 6-8: Fitting all models to spherical/conical/planar patch

In those experiments, the same conclusion about the superiority of fused data fitting is observed as in experiment 5. In general,fused data fitting yields a lower misclassification rate than surface-only fitting. The difference is more apparent when the noise level is high.

When fitting a spherical patch, we observed that among the wrong models, the conical model fitted the spherical surface patch the best when only surface data was used. This can be attributed to the fact that conical model has more degrees of freedom than the other models. However, with fused data, the curveness in contour data forces the conical model to be a bad fit. Instead, the planar model does better among the wrong models.

When fitting a conical patch, among the wrong models, the spherical model fit the conical patch the best if only surface data were used. With fused data, the cylindrical model would do better. Again, the straightness of the contour data eliminates the spherical model.

When fitting planar patches, as in the spherical case,conical model fares better (due to its higher degree of freedom)than the other wrong models when only surface data were fitted.When the contour data were added, none of the wrong models fit the planar patch well.

4.3 Simulation Results Summary

The simulation results of the first 4 experiments show that the use of fused data in surface parameter recovery is superior to using either the contour-only or the surface-only data.In general, the fused fit yields more accurate parameter estimates and better convergence rate (especially under higher noise level)without a significant increase in number of iterations before convergence. In fact, the average number of iterations for convergence went down using the fused data in some cases.

The Monte Carlo experiments directed toward recognition capability indicate that the proposed fused fitting method has a much lower false alarm rate than the method of fitting only surface data. On the rare occasions where the fit to an incorrect model does converge, the misclassification rate (wrong surface label) is also much lower. This misclassification rate appears to be small enough to give good input to our planned higher level scene reconstruction module. The observations made in each of the experiments strongly supports our hypothesis that edge contour information contributes greatly to the correct qualitative classification of surface shape.

5 Concluding Discussion

The novel idea of simultaneously fitting intensity contours and the adjacent range (surface) data is the central theme of this paper. We derived the contour equations of the limb projection of spheres, cylinders and cones from their respective 3D surface shape formulation and the projection of crease edges formed by intersecting quadric surfaces so that the 2D contour and 3D surface equation(s) are related by a common set of parameters. Furthermore, the true normal distance function between a data point and a particular surface/contour model was derived as the new residual function for least-squares fitting. We showed by means of the Monte Carlo experiments that (1) fused data fitting results in fewer bad fits and more accurate parameter estimates than if surface or contour data were used alone; (2) fused fitting is better able to discriminate the different surface types. The advantage of fused fitting was more evident when higher Gaussian noise was introduced in the experiments.

Finally, we should mention the fact that an algorithm for detecting *wing* primitives based on the simultaneous fitting of the contour and the surface data has been shown to be feasible in [16,15]. The wing dectection algorithm was tested on a variety of real images and the results concurred with the finding of our Monte Carlo experiments. As with any fitting problem, goodness of the initial fitting parameters is important to the success of the fit. We demonstrated in [15]

that the contour data plays a vital role in finding good starting values when the surface patch is small. Once again confirm our tenet that fused data fitting is superior than fitting either surface or contour data alone.

References

[1]R. Bajcsy and F. Solina. Three dimensional object representation revisited. In 1*st International Conference on Computer Vision*, pages 321-240, London, UK, June 1987.

[2]R. Bolle and D, Cooper. On optimally combining pieces of information, with application to estimating 3-D comples-object position from range data. *IEEE Transactions on Pattern Recognition and Machine Intelligence*, 8(5) :619-638, September 1986.

[3]R. M. Bolle, A. Califano, and R. Kjeldsen. A complete and extendable approach to visual recognition. *IEEE Transactions on Pattern Recognition and Machine Intelligence*, 14(5):534-548, May 1992

[4]X. Cao, N. Shrikande, and G. Hu. A comparison of quadric fitting methods for range data. Technical report, Center for Computer Vision and Rogotics Research, Department of Computer Science, Central Michitan University, September 1991.

[5]S. -W. Chen and G. Stockman. Object wings-21/2 D primintives for 3-D recognition. In *IEEE 1989 Conference on Computer Vision and Pattern Recognition*, pages 535-540, San Diego, CA, Jnue 1989.

[6]O. Faugeras, M. Hegert, and E. Pauchor. Segmentation of range data into planar and quadratic patches. In *IEEE 1983 Conference on Computer Vision and Pattern Recognition, pages* 8-13, Washington, D. C., June 198 3.

[7]M. A. Fischler and R. C. Bolles. Random sample consensus: A paradigm for model fitting with applications to image analysis and automated cartography. *Communications of the Association of Computing Madhinery*, 24(6):

381-395, June 1981.

[8]P. J. Flynn and A. K. Jain. Surface classification: Hypothesis testing and parameter estimation. In *IEEE 1988 Conference on Computer Vision and Pattern Recognition,* pages 261-267, Ann Arbor, MI, June 1988.

[9]A. D. Gross and T. E. Boult. Error of fit measures for recovering parametric solids. In *2nd International Confrernce on Computer Vision,* pages 690-694, Tampa, FL, December 1988.

[10]E. L. Hall, J, B, K, Tio, C. A. McPherson, and F, A, Sadjadi. Measuring curved surfaces for robot vision. *IEEE Computer,* 15(12):42-54, December 1992.

[11]D. Keren, J. Subrahmonia, and D. B. Cooper. Robust object recognition based on implicit algebraic curves and surfaces. In *IEEE 1992 Conference on Computer Vision and Pattern Recognition,* Pages 791-794, Champaign, IL, June 1992.

[12]J. J. Koenderink. What does the occluding contour tell us about solid shape ? *Perception,* 13:321-330, 1984.

[13]D. J. Kriegman and J. Ponce. On recognizing and positioning curved 3-D objects from image contours. *IEEE Transactions on Pattern Recognition and Machine Intelligence,* 12(12):1127-1137, December1990.

[14]P. Lancaster and K. Salkauskas. *Curve and Surface Fitting.* Acadimic Press, San Diego, CA, 1986.

[15]G. C. Lee. *Reconstruction of Line Drawing Graphs from Fused Range and Intensity Imagery.* PhD thesis, Michigan State University, 1992.

[16]G. C. Lee and G. C. Stockman. Detecting object wings in quadric surface scenes. In *SPIE 1708:Applications of Artificial Intelligence X: Machine Vision and Robotics, Pages* 335-344, Orlando, El, April 1992.

[17] D. G. Lowe. Three-dimensional object recognition from single two-dimensional. images *Artificial Intelligence,* 31:355-395, 1987.

[18]D. G. Lowe. Fitting parameterized three-dimensional models to images. *IEEE Transactions on Pattern Recognition and Machine Intelligence,* 13(

5):441-450, May 1991.

[19]D. Marr and H. Nishihara. Representation and recognition of the spatial organization of three-dimensional shapes. *Proceedings of Royal Society of Londom*, 200:269-294, 1977.

[20]Y. Muller and R. Mohr. Planes and quadrics detection using Hough Transform. In *7th International Conferece on Pattern Recognition, pages* 1101-1103,Montreal, Canada, July 1984.

[21]A. Pentland.Recognition by parts.In *1st International Coference on Computer Vision* , pages 621-620, London, Uk, June 1987.

[22]W. Press, B. Flannery, S. Teukolsky, and W. Vetterling, editors. *Numerical Recipes in C: THE Art of Scientific Computing.* Cambridge University Press, Cambridge, England, 1988.

[23]F. Solina and R. Bajcsy. Recovery of parametric models from range images: The case for superquadrics with global deformations. *IEEE Transactions on Pattern Recognition and Machine Intelligence,* 12(2): 131-147, February 1990.

[24]G. Taubin. Estimation of planar curves, surves, surfaces, and nonplanar sarface curves defined gy implicit equations with applications to edge and range image segmentation. *IEEE Transactions on Pattern Recognition and Machine Intelligence,* 13(11):1115-1138, November 1991.

[25]Technical Arts Corporation. *100X 3-Dimensional Scanner: User's Manual and Application Programming Guide.* Redmond, Washington.

經由邊界及表面同時調適的方式重建二次曲面形狀

李忠謀

國立臺灣師範大學資訊教育研究所

摘　要

本文提供的技巧，可以用來從對應的光度及景深影像中，偵測出二度物體的子部位形狀。主要的假設包括：(1)物體最突顯的特徵乃是發生在物體的輪廓部位以及物體表面上的邊線，(2)物體可能有互相遮掩的情形，故重建物體的形狀只能藉重於物體較小的部位。本文所提供的方法，乃是經由將線條及表面的資料，同時調適，使得以匹配二次曲面形式的一種技巧。所須要使用的圓球、圓柱及圓錐二次曲面結合邊線的方程式在文中均有推導。藉蒙地卡羅方式的測驗，我們得以證實：(1)線條及表面資料同時調適的結果，以調適的品質來看，會優於個別調適的方式；(2)利用對應光度及景深影像資料來偵測物體的形狀，可以降低物體表面錯誤分類的發生。